COMBINED LDA-CARS MEASUREMENTS OF VELOCITY-TEMPERATURE CORRELATIONS IN TURBULENT FLAMES

M.J. Tummers, E.H. van Veen, N. George, R. Rodink, and K. Hanjalić
Delft University of Technology
Faculty of Applied Sciences
Section Thermal and Fluids Sciences
P.O. Box 5046, 2600 GA Delft, The Netherlands

ABSTRACT

Simultaneous measurements of velocity and temperature were conducted in a turbulent jet diffusion flame. Temperatures were measured by using Coherent Anti-Stokes Raman Spectroscopy (CARS) whereas Laser Doppler Anemometry (LDA) was used for the velocity measurements. The temperature and velocity samples were processed to form (time-dependent) velocity-temperature correlation functions. The measured correlation functions indicated that the gradient-diffusion hypothesis is reasonably accurate for the radial direction. However, for the axial direction the gradient diffusion hypothesis is accurate only in the central region of the flame while counter-gradient diffusion is found in the outer region.

INTRODUCTION

Reynolds averaging of the energy equation gives rise to the Reynolds fluxes, $\overline{T'u'}$, $\overline{T'v'}$, and $\overline{T'w'}$. These correlations between turbulent velocity and temperature fluctuations are unknowns that have to be modeled, i.e. expressed in terms of known quantities, in order to close the set of equations. In computational studies of turbulent flames it is common to use a gradient-type model for the velocity-temperature correlations. In other words, it is assumed that $\overline{T'u'} = -D_t \partial\overline{T}/\partial x$, where D_t is a turbulent diffusivity. It is widely known, however, that gradient-type models can be inaccurate in flows with swirl or large-scale turbulence. The inaccuracy of the gradient hypothesis can be so large that even the sign of the flux is predicted wrong. In that case it is said that counter-gradient transport occurs.

Accurate experimental data on Reynolds fluxes gives insight in the transport of heat in turbulent flames and may help to develop and validate models that are used in computational methods. However, most existing experimental data on turbulent heat fluxes in flames were obtained from measurement techniques that make use of a physical probe. Ideally, one would use only optical techniques to measure the heat fluxes. The major advantage of optical methods is that they make it possible to perform measurements in a purely non-intrusive manner, thereby leaving the flow field unaffected. Some of the optical techniques of choice are Laser Doppler Anemometry (LDA) for flow characterization whereas Raman-Rayleigh scattering and Coherent Anti-Stokes Raman Spectroscopy (CARS) can be used to extract the temperature. Individually, these techniques are well developed and their use is widespread, but joint measurements of velocity and temperature are seldom reported.

One interesting duet is the integrated CARS/LDA system. The advantage of CARS over Raman-Rayleigh spectroscopy is the coherent nature of the CARS signal, which enables the probing of the luminous, yellow regions of flames. To the author's knowledge, there are only two earlier reports on the combined use of LDA and CARS, i.e., Fujii et al. (1984) and Goss et al. (1989). Unfortunately, after the preliminary measurements reported by Fujii et al. (1984) and a still improved version by Goss et al. (1989), this approach was almost in a dormant state with no further developments.

This paper reports on the use of an integrated LDA/CARS system for measuring velocity-temperature correlations in luminous turbulent diffusion flames. The major difference between the work reported by Goss et al. (1989) and the present investigation is that the latter uses the information on the lag time between velocity and temperature samples to determine the time-dependent velocity-temperature correlation function instead of focusing only on the value of this correlation function at zero lag time. The measured correlation functions are used to study the occurrence of counter-gradient diffusion in the outer region of a jet diffusion flame.

TEST CONFIGURATION

A natural-gas fired burner was used to produce a well-defined axi-symmetric turbulent diffusion flame. The burner consists of two concentric pipes each having a length of 1 m. The center jet provides the fuel while the annulus provides the primary air, see Fig. 1. The initial diameter of the central fuel pipe is 8 mm, but a pilot-flame insert placed in the exit of the fuel pipe causes a decrease of the diameter to 6 mm starting at a position 16 mm upstream of the nozzle exit. The fuel stream is separated from the annular air stream by a 4.5 mm wide ring on which pilot flames can be operated. However, the pilot flames were not used in this study. Instead, the flame was stabilized by the small backflow region located directly above the ring.

The air annulus has an outer diameter of 45 mm. The inner diameter of the air annulus is 30 mm over the first 940 mm of the pipe. The inner diameter then decreases to 15 mm in the final 60 mm, which gives rise to a small negative radial velocity of the air at the burner exit. The fuel velocity was 21.9 m/s and the air velocity was 4.4 m/s, resulting in Reynolds numbers for the fuel and air jet of 9700 and 8800, respectively. Dutch natural gas was used with the following molar composition of the major components: 81.3 % CH_4, 2.9 % C_2H_6 and 14.3 % N_2.

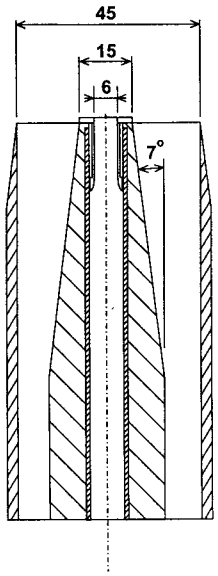

Figure 1: Cross-section of the natural-gas diffusion burner.

Throughout this paper, a coordinate system will be used with its origin at the burner exit plane. The x-coordinate is measured along the axis of the burner and r denotes the radial coordinate.

EXPERIMENTAL TECHNIQUE

CARS system

The CARS experimental set-up is sketched in Fig. 2. The system is based on a frequency-doubled Nd:YAG laser (Continuum YA-680), which yields 400 mJ per pulse at 532 nm (ω_1 = 18.8 x 10^3 cm^{-1}) with a pulse duration of 6 ns at a 10 Hz repetition rate. About 80 % of the ω_1 radiation is used to pump a broadband dye laser (Continuum TDL-60). By using Rhodamine 640 dye in methanol, the resulting Stokes radiation has a central wavelength of 607 nm (ω_2 = 16.5 x 10^3 cm^{-1}). The remaining 20 % of the ω_1 radiation is split to form two equal intensity pump beams. The three beams are arranged according to the folded BOXCARS phase-matching scheme and focused inside the flame by using a 350 mm focal length lens. The CARS measuring volume has a diameter of 0.05 mm and a length of 0.9 mm.

The generated CARS radiation ($\omega_3 = 2\omega_1 - \omega_2$) is re-collimated and spectrally dispersed in a SPEX-1404 0.85 m double spectrometer. The N_2 ro-vibrational spectrum (Q-branch) is recorded on a CCD detector (Princeton Instruments TE/CCD-1100P) with 1100 x 330 pixels. The pixels are binned in the vertical direction to yield a read-out array of 1100 intensity values, which are digitized by an 18-bit AD-converter and stored. With the multimode Nd:YAG laser (1 cm^{-1} line width) and the 0.3 cm^{-1} dispersion of the spectrometer over the detector pixels, the instrument function determining the spectral resolution is a 1.25 cm^{-1} wide Gaussian function. This instrument function is used to compute a convolution of the theoretical ro-vibrational spectra for a large number of temperatures ranging between 300 K and 2200 K. A measured instantaneous temperature follows from a best-fit comparison between a measured ro-vibrational spectrum and the set of convoluted theoretical spectra.

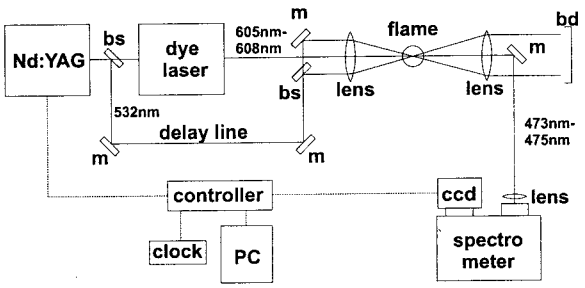

Figure 2: CARS instrumentation for observing the N_2 Q-branch. (Abbreviations: m=mirror, bs=beam splitter, bd=beam dump.)

LDA system

Turbulent velocity fluctuations were measured with a one-component, fibre-optic Dantec LDA system using the green (514.5 nm) color of a 4 W argon-ion laser (Spectra Physics 2016), see Fig. 3 for details. The two intersecting laser beams were oriented such that either the streamwise or the radial velocity component was measured directly. One laser beam was frequency shifted over 40 MHz by an acousto-optic Bragg cell to enable the detection of instantaneous flow reversals. Both laser beams were passed through separate beam expanders before intersecting. The length and diameter of the measuring volume were 0.9 mm and 0.1 mm, respectively. Scattered light was collected in a 10° off-axis, forward direction with a 110 mm aperture lens, and then focused on a photomultiplier. The photomultiplier output signal was electronically down-mixed to an effective pre-shift of 5 MHz and subsequently fed to a TSI IFA-750 signal processor.

Aluminum oxide (Al_2O_3) particles with an average diameter of about 1 μm were used as seed particles. Two cyclone-type particle generators were used to seed the air and fuel flows separately.

Integration of CARS and LDA

The spatial coincidence of the CARS and LDA measuring volumes was achieved by using a fine aperture with a diameter that was slightly less than that of the probe volumes. The individual CARS and LDA systems did not have common optical components and could be operated independently. The integration of both instruments is largely determined by the time logic used for the acquisition of "simultaneous" temperature and velocity samples. The CARS instrument takes temperature samples at regular time intervals of about 100 ms, i.e., whenever the Q-switch of the Nd:YAG laser fires. On the other hand, the

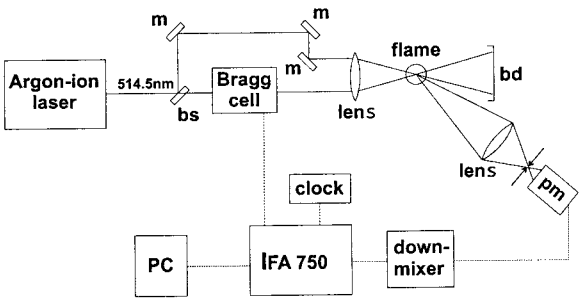

Figure 3: LDA instrumentation for measuring the radial or the axial velocity component.

LDA system samples the velocity only when a light-scattering particle moves through the measuring volume. Since the particles are randomly distributed in space, the sampling times are random as well. As explained by Goss et al. (1989), the problem of integrating CARS and LDA lies in the synchronization of an equidistant and a random sampling process. In the present investigation a simple but robust method was adopted for the synchronization. In essence, both the CARS system and the LDA system run independently and a common clock (with 2 μs resolution) was used to tag the temperature and velocity data with time. A computer program was then used to compute the lag time τ between temperature and velocity samples. The samples were subsequently used to determine the velocity-temperature correlation functions $\rho_{Tu}(\tau)$ and $\rho_{Tv}(\tau)$, i.e.,

$$\rho_{Tu}(\tau) = \frac{\overline{T'(t)u'(t+\tau)}}{(\overline{T'^2}\,\overline{u'^2})^{1/2}}, \qquad (1)$$

and

$$\rho_{Tv}(\tau) = \frac{\overline{T'(t)v'(t+\tau)}}{(\overline{T'^2}\,\overline{v'^2})^{1/2}}, \qquad (2)$$

where u' and v' are velocity fluctuations in the axial and radial direction, respectively.

Data processing for combined CARS/LDA measurements

Due to the random sampling times in LDA, a discretized version of the velocity-temperature correlation function is computed, similar to Mayo's slotting method (Mayo [1974]) for the calculation of velocity autocorrelation functions. In mathematical terms, the slotted velocity-temperature correlation function $\rho_{Tu}(\tau)$ followed from

$$\rho_{Tu}(k\Delta\tau) = \frac{\sum T_i' u_j'(k\Delta\tau)}{(\sum T'^2(k\Delta\tau)\sum u'^2(k\Delta\tau))^{1/2}}, \qquad (3)$$

with $|k| = 0,1,...,M$. In this expression $\sum T_i' u_j'(k\Delta\tau)$ is the sum of all products $T'(t_i)\,u'(t_j)$ having a lag time $\tau = t_j - t_i$ within the interval $k\,\Delta\tau < t_j - t_i < (k+1)\,\Delta\tau$. The slot width $\Delta\tau$ is determined from $\Delta\tau = \tau_m/(M+1)$, where $2M+1$ is the number of slots and τ_m is the maximum (positive) lag time. Note that the lag time is assumed to be positive when a velocity sample is taken after measuring a temperature. The Reynolds flux, $\overline{T'u'}$, follows from the value of the correlation coefficient at zero lag time, i.e. the value of ρ_{Tu} for either k=-1 or k=0, multiplied by the product of the rms values of temperature and velocity, $(\overline{T'^2}\,\overline{u'^2})^{1/2}$. The average number of products $T'(t_i)\,u'(t_j)$ per slot is given by

$$H(k\Delta\tau) = N\nu\Delta\tau, \qquad (4)$$

with $|k| = 0,1,...,M$. In this expression, N is the total number of temperature samples and ν is the mean rate at which velocity samples are collected. The velocity-temperature products $T'(t_i)\,u'(t_j)$ in the intervals for k=-1 and k=0 can be considered "time coincident" when there is negligible change in the velocity during time span $\Delta\tau$. This means that the velocity autocorrelation $\rho_{uu}(\tau)$ should be nearly 1 at a lag time equal to $\Delta\tau$ so that $\Delta\tau$ should be roughly equal to the Kolmogorov time scale. As a consequence, the total number of velocity-temperature products is low unless very large amounts of data are collected. The velocity autocorrelation function was computed from the locally scaled version of the slotting method, i.e.,

$$\rho_{uu}(k\Delta\tau) = \frac{\sum u_i' u_j'(k\Delta\tau)}{(\sum u_i'^2(k\Delta\tau)\sum u_j'^2(k\Delta\tau))^{1/2}}, \qquad (5)$$

with $k = 0,1,...,M$-1. The lag times $t_i - t_j$ are in the interval $(k\text{-}1/2)\,\Delta\tau < t_i - t_j < (k+1/2)\,\Delta\tau$. Note that the slot centers for the velocity autocorrelation are shifted over $\Delta\tau/2$ with respect to the slot centers for the velocity-temperature correlation. The local scaling is applied to reduce the statistical scatter of the velocity autocorrelation values for small lag times, i.e., when the velocity autocorrelation is near 1.

RESULTS AND DISCUSSION

Correlation functions

The velocity-temperature correlation function measured at x=150 mm and r=8 mm is given in Fig. 4. This function was constructed using approximately 2.4 x 10^4 temperature samples that were acquired during a 2500 s measurement run. The LDA system collected about 3.04 x 10^6 velocity samples during this run. The temperature and velocity samples, together with the time information, were then processed using Eq (3) with 120 slots, each having a width of 100 μs. The relatively high scatter of the correlation coefficients in Fig. 4 is caused by the limited number of velocity-temperature products, $T'(t_i)v'(t_j)$, per slot. Each slot contained about 2800 velocity-temperature products in good agreement with the theoretical value given by Eq (4). The correlation between velocity and temperature is essentially zero for (absolute values of) lag times τ larger than about 2 ms. Unlike velocity autocorrelation functions, the velocity-temperature correlations are generally not even in the lag time τ, and the maximum (or minimum) value is not always located at zero lag time.

Inspection of a large number of measured velocity-temperature correlation functions indicated that the first correlation coefficient with positive lag time, i.e. the data point for k=0 in Eq (3), is frequently 'out-of-line' with its neighboring data points. It is believed that this is the result of an undesired effect of CARS on LDA. For this reason the first correlation coefficient with positive lag time (k=0)

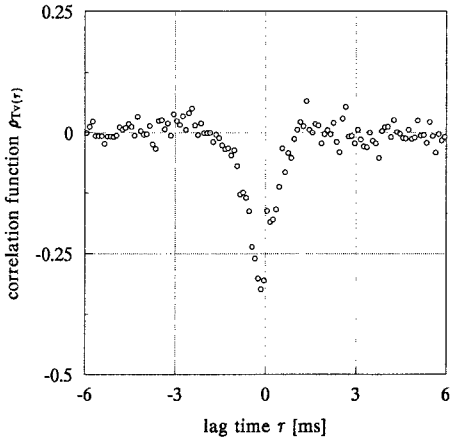

Figure 4: Velocity-temperature correlation function $\rho_{Tv}(\tau)$ measured at x=150 mm, r=8 mm.

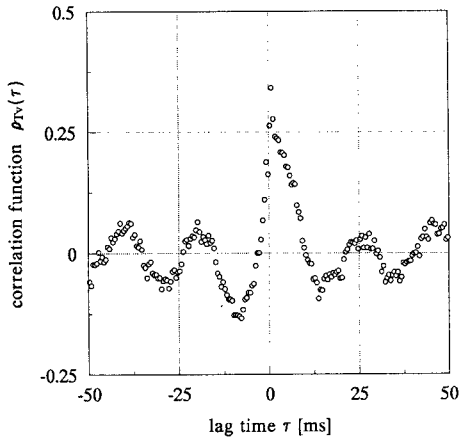

Figure 5: Velocity-temperature correlation function $\rho_{Tv}(\tau)$ measured at x=150 mm, r=18 mm.

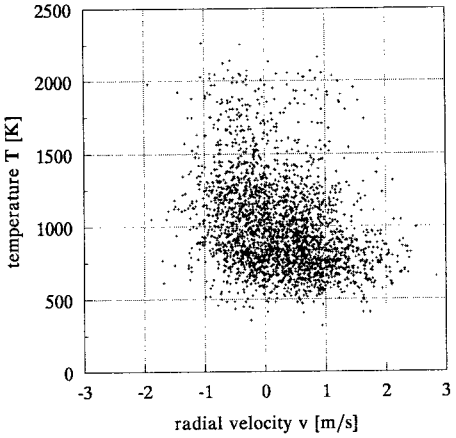

Figure 6: Instantaneous temperature versus instantaneous radial velocity at x=150mm, r=8mm.

was not used in the estimation of the value of the correlation coefficient at zero lag time. Instead, this coefficient was determined from the measured correlation coefficient for k=-1. For the measurements shown in Fig. 4 this means $\overline{T'v'}/(\overline{T'^2}\,\overline{v'^2})^{1/2} \approx -0.31$.

Validity of the gradient-diffusion hypothesis

The velocity-temperature correlation function $\rho_{Tv}(\tau)$ shown in Fig. 5 was measured at position x=150 mm, r=18 mm, where the flame has a large scale, quasi-periodic behavior. Note that the lag-time axis in this graph spans a range of 100 ms, which is much larger than the range in Fig. 4 (12 ms). The correlation function $\rho_{Tv}(\tau)$ depicted in Fig. 5 yields a correlation coefficient at zero lag time of about 0.25. The sign of this correlation coefficient is opposite to that of the correlation coefficient measured in r=8 mm. For the measurement in r=8 mm, the "time-simultaneous" velocity and temperature samples from slot k= -1 are shown in Fig. 6. Similar results for the measurement in r=18 mm are given in Fig. 7. In both scatter plots the temperature varies between room temperature and a maximum of 2250 K, which is close to the adiabatic flame temperature for stoichiometric natural-gas/air combustion.

The radial position r=8 mm is on the fuel side of the mean-temperature maximum, so that a positive radial velocity fluctuation (v' >0) brings cold material into a hot region which causes a negative temperature fluctuation, i.e. T' <0. On the average this produces the negative correlation between temperature and radial velocity fluctuations observed in the scatter plot. Note that the negative sign of the correlation coefficient is in agreement with the gradient-diffusion hypothesis. On the other hand, r=18 mm is located on the air side of the mean-temperature peak. In this case, a positive radial velocity fluctuation (v' >0) transports hot material to a colder region, i.e., T' >0, thereby producing a positive correlation between the fluctuations in temperature and radial velocity. This is again in qualitative agreement with the gradient-diffusion hypothesis.

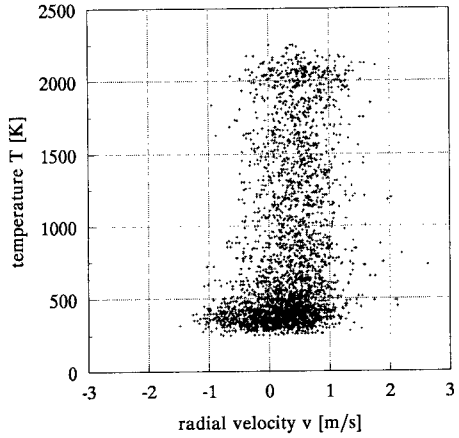

Figure 7: Instantaneous temperature versus instantaneous radial velocity at x=150mm, r=18mm.

The above results for r=8 mm and r=18 mm strongly suggest that the gradient-diffusion hypothesis can be used to predict at least the sign of the velocity-temperature correlation coefficients. This was investigated further by measuring correlation coefficients at a number of other radial positions. Figure 8 shows the distribution of the radial correlation coefficients ρ_{Tv} (0) measured at station x=150 mm. Also shown is the mean-temperature gradient in the radial direction measured at this station. The minimum value of the correlation coefficient (ρ_{Tv} (0) ≈ -0.31) is found in the region where the temperature gradient has its largest value. Furthermore, the measured correlation coefficient is nearly zero on the symmetry axis, and changes sign near r=13.5 mm where the mean temperature has a maximum. This indicates that there is good qualitative agreement between the measured correlation coefficients and the gradient-diffusion hypothesis for the radial direction.

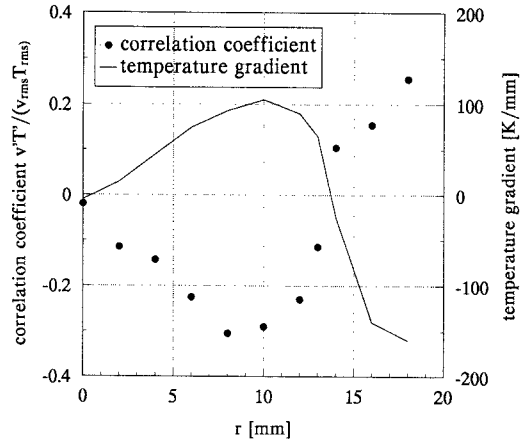

Figure 8: The correlation coefficient $\overline{T'v'}/(\overline{T'^2}\,\overline{v'^2})^{1/2}$ and the radial mean-temperature gradient $\partial\overline{T}/\partial r$ at station x=150 mm.

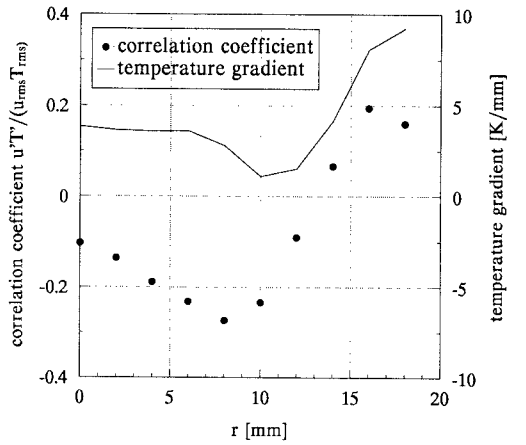

Figure 9: The correlation coefficient $\overline{T'u'}/(\overline{T'^2}\,\overline{u'^2})^{1/2}$ and the axial mean-temperature gradient $\partial\overline{T}/\partial x$ at station x=150 mm.

At station x=150 mm the mean-temperature gradient in the x-direction is positive for all values of the radial coordinate r as depicted in Fig. 9. According to the gradient-diffusion hypothesis the axial correlation coefficient ρ_{Tu} should be negative for all values of r. This is indeed the case for the central region of the flame. However, the measurements reveal that ρ_{Tu} is positive in the outer region indicating counter-gradient transport.

To find the cause of the counter-gradient transport in the present jet diffusion flame, attention will be directed to the large scale, quasi-periodic behavior that occurs in the outer region of the flame. Figure 10 shows the autocorrelation functions of the radial velocity component in r=8 mm and r=18 mm. The autocorrelation for r=8 mm falls off rapidly with increasing lag time without any sign of a periodicity indicative of small scale turbulence. In contrast, the autocorrelation for r=18 mm has a much larger time scale and an oscillation with a frequency of approximately 45 Hz. Figures 11 and 12 depict the velocity-temperature correlation for the axial direction,

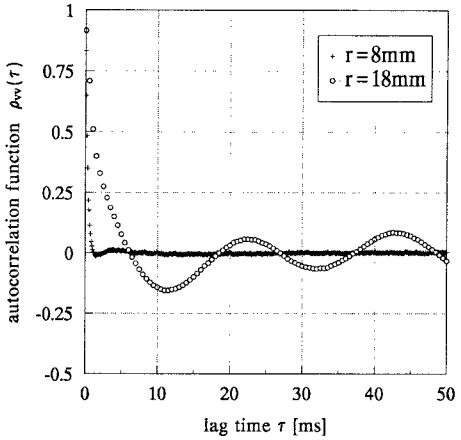

Figure 10: Autocorrelation functions measured at r=8mm and r=18mm.

$\rho_{Tu}(\tau)$, measured at r=8 mm and r=16 mm, respectively. The latter position is located on the air-side of the mean-temperature peak, like position r=18 mm. The velocity-temperature correlation measured in r=8 mm is negative at zero lag time (in agreement with the gradient-diffusion hypothesis) and goes to zero rapidly. On the other hand, the velocity-temperature correlation, $\rho_{Tu}(\tau)$, in r=16 mm is positive at zero lag time (indicating counter-gradient transport), and has a much larger time scale than that in position r=8 mm. Apparently, there is a large scale motion on the air-side of the mean temperature peak. This motion causes a periodicity in the radial velocity component, but not in the axial velocity component.

The large-scale motion is caused by the quasi-periodic formation of, so-called, flame bulges, which were visualized by using an intensified high-speed camera (HI-CAM produced by Lambert Instruments) that recorded the flame luminosity. During a measurement run, the HI-CAM collected 512 images (256 x 1024 pixels) at a rate of 1828 fps each with an exposure time of 10 μs. Figure 13 depicts a sequence of seven images with an inter-frame time of 1641μs, because only every third image is shown here. The images show the luminosity in a region of approximately

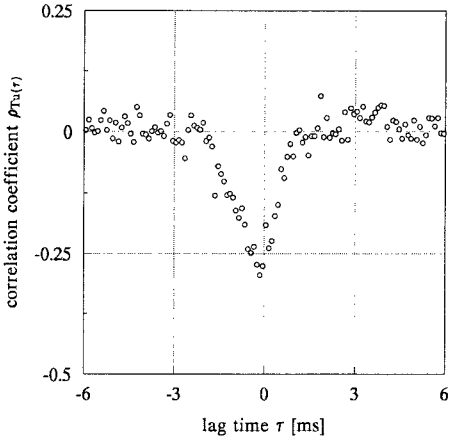

Figure 11: Velocity-temperature correlation function ρ_{Tu} (τ) measured at x=150 mm, r=8 mm.

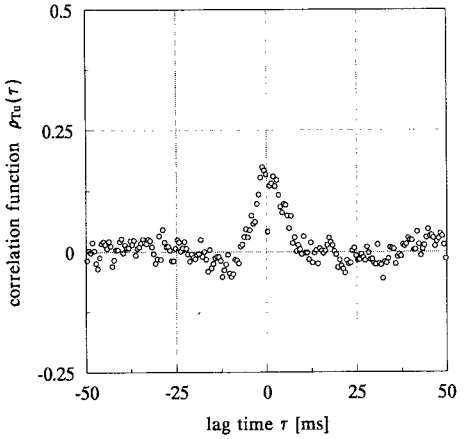

Figure 12: Velocity-temperature correlation function $\rho_{Tu}(\tau)$ measured at x=150 mm, r=16 mm.

60 x 230 mm^2 with the burner exit visible at the bottom. In the upper left of the images a flame bulge is seen to develop while the flame is squeezed just above the bulge. The bulge moves upward with a velocity of approximately 8 m/s. Following the ideas of Chen et al. [1988], the flame bulge is formed through the interaction of the flame with large toroidal vortices that originate from the (outer) shear layer between the primary air and the ambient. These external vortices should not be confused with the smaller vortices that develop in the (inner) shear layer of the fuel jet and the primary air. The bulge is formed when a large external vortex just below the bulge moves material radially outward, while the vortex above the bulge moves material inwards thus squeezing the flame. Analyses of two movies each with 514 images showed that the formation of flame bulges coincides well with the 45Hz quasi-periodicity that was detected from the single-point CARS/LDA measurements. If a flame bulge moves over the CARS/LDA measuring volume, then hot material (T'>0) with a relatively high axial velocity (u'>0) is transported radially outward (v'>0). Such an event strongly promotes positive correlation coefficients for both the radial and the axial directions. In the latter case the positive value for the correlation coefficient will be interpreted as counter-gradient transport.

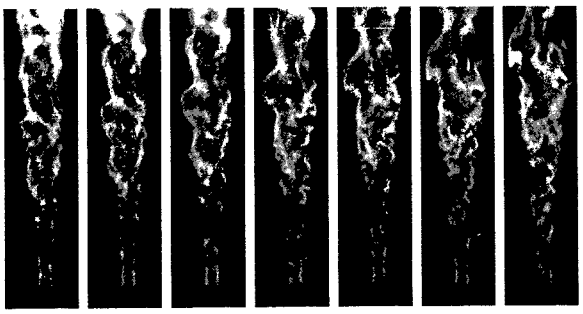

Figure 13: Sequence of flame luminosity images of the turbulent jet diffusion flame.

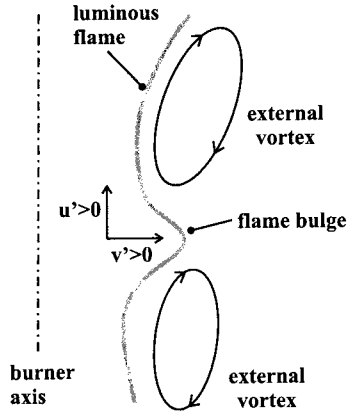

Figure 14: Formation of a flame bulge, and its effect on the radial and axial temperature-velocity correlations.

CONCLUSIONS

An integrated CARS/LDA instrument for simultaneous temperature and velocity measurements has been described. This instrument was used to measure time-resolved velocity-temperature correlation functions, and turbulent heat fluxes in a jet diffusion flame. The results indicated that the gradient-diffusion hypothesis was accurate for the radial direction, but for the axial direction counter-gradient diffusion was found to occur in the outer region of the flame. The counter-gradient diffusion is a consequence of a large scale, quasi-periodic motion caused by the presence of flame bulges in the outer region of the flame. The large-scale motion results in large positive values for the correlation between temperature and velocity fluctuations for both the radial and the axial direction. The latter is interpreted as counter-gradient diffusion.

REFERENCES

Chen L D; Seaba J P; Roquemore W M; Goss L P (1988) Buoyant diffusion flames. Proc of the 22nd Symp on Combustion. pp.677-684

Fujii S; Gomi M; Eguchi K; Yamaguchi S; Jin Y (1984) Time resolved LDV and CARS measurements in a premixed reacting flow. Combust. Sci. Technol. 36:211-226

Goss L P; Trump D D; Lynn W F; Chen T H; Schmoll W J; Roquemore W M (1989) Second-generation combined CARS-LDV Instrument for simultaneous temperature and velocity measurements in combusting flows. Rev. Sci. Instrum. 60(4):638-645

Mayo W T (1974) A discussion of limitations and extensions of power spectrum estimation with burst counter LDV systems. Proc. 2nd Intl Workshop on Laser Velocimetry, Purdue University, pp. 90-104